Studies of Particle Dispersion in Plasticized Poly(vinyl chloride)/Montmorillonite Nanocomposites

A. L.G. Saad,[1] O. I. H. Dimitry[2]

[1]*Academy of Scientific Research, Microwave Physics Department, National Research Centre, Cairo, Egypt*
[2]*Academy of Scientific Research, Petrochemicals Department, Egyptian Petroleum Research Institute, Cairo, Egypt*

Received 20 June 2010; accepted 2 November 2010
DOI 10.1002/app.33807
Published online 16 August 2011 in Wiley Online Library (wileyonlinelibrary.com).

ABSTRACT: Poly(vinyl chloride)(PVC) and dioctyl phthalate (DOP) were mixed with 5 and 10 wt % of Cloisite Na^+, Cloisite 30B or Cloisite 93A. The obtained nanocomposites were characterized by thermal analysis using a thermogravimetric analyzer which showed that addition of 5 wt % of nanoclay to PVC increased its thermal stability in the sequence: Cloisite Na^+< Cloisite 93A< Cloisite 30B. The electrical conductivity of these composites was studied as a function of temperatures and showed that the conductivity of PVC was enhanced upon using 5 wt % of nanoclay in the sequence: Cloisite Na^+< Cloisite 30B < Cloisite 93A. The activation energy of interaction of PVC with nanoclay was found to be lowest for the composite containing 5 wt % of nanoclay in the same sequence. The tensile strength, elongation (%), and Young's modulus were considerably enhanced upon increasing the clay content to 5 wt % in the sequence: Cloisite Na^+< Cloisite 93A < Cloisite 30B. X-ray diffraction (XRD) and scanning electron microscopy (SEM) were used to study these nanocomposite structures, and it was found that the organoclay layers are homogeneously dispersed in the PVC matrix when 5 wt % of Cloisite 30B or Cloisite 93A was used. J Appl Polym Sci 123: 1407–1420, 2012

Key words: poly(vinyl chloride); nanoclay; nanocomposite; montmorillonite; electrical conductivity; mechanical properties; exfoliation; intercalation

INTRODUCTION

Filling polymers with particles has been widely used as a method of improving the mechanical properties of the resulting composite materials, such as heat distortion temperatures, hardnesses, toughnesses, and mold shrinkages, as well as their fire resistances and electrical, and thermal conductivities, especially at high filler contents (sometimes >50 wt %).[1]

Polymer nanocomposites represent a new class of composite materials,[2,3] i.e., particle-filled polymers in which at least one dimension of the dispersed particles (i.e., length, width, or thickness) is in the nanometer range. Therefore, more interfacial interactions between the nanoparticles and the polymer matrix are expected. This will lead to improved properties for the related composite materials at much lower filler contents; for instance 3–5 wt % of nano-sized filler gives comparable properties to those obtained for 30–50 wt % of micron-sized filler.[4] The most successful results have been obtained when using layered silicates (Fig. 1) as nanofiller precursors, especially montmorillonite[5,6] (MMT), a mica-type silicate that consists of sheets arranged in a layered structure. It is used due to its high achievable surface area (about 750 m^2/g), its platelet thickness of 1 nm, and its high cation exchange capacity.[7] To improve its compatibility with the polymer, the intergallery cations (e.g., Na^+) of the layered silicate can be replaced with suitable alkyl ammonium salts acting as organic modifiers. By mechanically mixing it with the polymer matrix, this organically modified clay can be dispersed into small silicate stacks, or even into single platelets with a high aspect ratio. The resulting nanocomposites show large improvements in barrier properties,[8] flame resistance,[9] and dimensional stability, as well as in mechanical properties such as tensile strength, tensile modulus, and heat distortion temperature, without any significant loss of optical transparency, toughness, and impact strength.[5,10]

Nanostructured polymers have received much attention in the field of material sciences because of their unique mechanical, optical, electrical, and magnetic properties, and their applications in nano-materials and nanodevices. One of the main research and development domains in which they are used is the fabrication of nanocomposites for the electronics industry, where the rapid progress in computing technology always demands smaller components. Nano-technology utilizes objects with particle sizes from below one and up to hundreds of nanometers.[11]

The literature contains numerous studies concerning polymer nanocomposites based on various polymer matrices, such as nylon 6, epoxy resin,

Correspondence to: O. I. H. Dimitry (onsy_dimitry@hotmail.com).

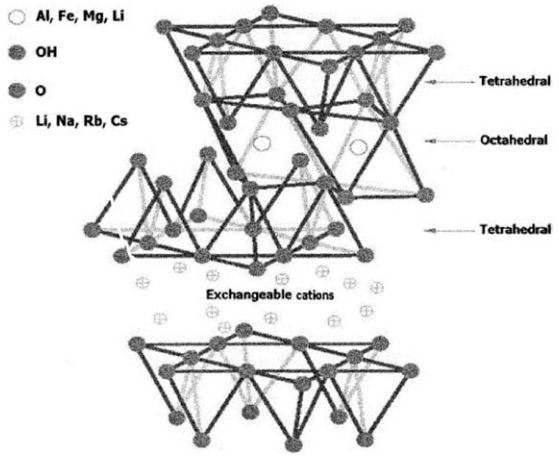

Figure 1 The structure of a layered silicate.

polystyrene, polypropylene, polyethylene, poly(ethylene oxide), polyimide, poly(methyl- methacrylate), polyurethane, and others.[12,13]

Although poly(vinyl chloride) (PVC) is one of the most largely used thermoplastics, only little attention has been paid to PVC/layered silicate nanocomposites.[14,15] However, due to its inherent disadvantages, such as low thermal stability and brittleness, it is necessary to develop new PVC products with high quality and good properties by introducing nanofillers to yield high added values and broaden PVC applications. PVC is a polar polymer; therefore, it is more convenient to use a polar modified type of clay. Dioctyl phthalate (DOP) which is a common plasticizer for PVC, is favorable to the intercalation process, consistent with the swelling of the clay by this plasticizer (increased interlayer distance).

This article describes preparation of three kinds of PVC/MMT nanocomposites and thermal stability investigation of the obtained products. The effects of adding 5 and 10 wt % of nanofiller particles on the electrical properties (permittivity, dielectric loss, and electrical conductivity) as well as the mechanical properties (tensile strength, elongation (%), and Young's modulus) of plasticized PVC are also examined. The study of the activation energy of interaction of PVC with nanoclay has been carried out. Furthermore, morphological studies of PVC nanocomposites have been conducted using X-ray diffraction (XRD) and scanning electron microscopy (SEM) techniques.

EXPERIMENTAL

Materials

In this work, montmorillonite (MMT) obtained from Southern Clay Products (Gonzales, TX) was used as nanofiller. Its silicate layers are approximately 200 nm long and 1 nm thick, and the interlayer spacing between its stacked layers, denoted d_{001}, is about 1 nm.[16] Two different types of MMT were used: Cloisite Na^+, a natural MMT modified for higher Na content and two organophilic MMTs, Cloisites 30B and 93A, which are types of Cloisite Na^+ that has been modified with two different quaternary ammonium salts. Cloisite 30B contains methyl tallow bis-2-hydroxyethyl ammonium cations, at a loading of 90 meq/100g clay (Fig. 2), where tallow is $\sim$ 65% $C_{18}H_{37}$; $\sim$ 30% $C_{16}H_{33}$; $\sim$ 5% $C_{14}H_{29}$. Cloisite 93A contains methyl dihydrogenated tallow ammonium cations at a loading of 90 meq/100 g clay (Fig. 3), where tallow is $\sim$ 65% $C_{18}H_{37}$; $\sim$ 30% $C_{16}H_{33}$; $\sim$ 5% $C_{14}H_{29}$.

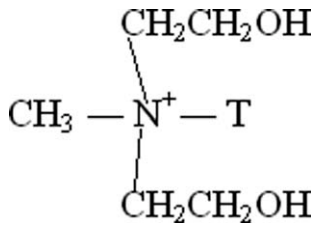

Figure 2 Chemical modifier of Cloisite 30B.

The suspension type of poly(vinyl chloride) (PVC) (K value 67) (100 parts) was used as polymer matrix. Dioctyl phthalate (DOP) (40 parts) was used as PVC plasticizer and dibutyltindilaurate (three parts) as a heat stabilizer.

Preparation of PVC/MMT nanocomposites

Poly(vinyl chloride) (PVC) and dioctyl phthalate (DOP) plasticizer were mechanically mixed with 5 and 10 wt % of Cloisite Na^+, Cloisite 30B, or Cloisite 93A and then compounded in Buss KO-kneader MKS 30 single screw extruder. Compounding was carried out at 130-160°C using a screw speed in the range of 25 to 45 rpm. Nanocomposites extrudates were thereafter palletized for calendaring.

Methods of testing

Thermogravimetric analysis

Thermogravimetric analysis (TGA) was conducted on a TGA7 thermal analysis system of Perkin–Elmer Co. at a heating rate of 10°C/min under a flowing

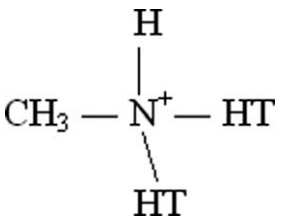

Figure 3 Chemical modifier of Cloisite 93A.

nitrogen atmosphere. The temperature scan ranged from 50 to 700°C.

Dielectric measurements

The permittivities (ε′) and dielectric losses (ε″) of the prepared samples were measured at different frequencies ranging from 100 Hz to 100 kHz. An Ando Electric (Tokyo, Japan) LCR meter (type AG-4311B) with an NFM/5T test cell (Wiss.Tech.Werkstatten, Weilheim, Germany) was used. The capacitance C and the loss tangent (tan δ), from which ε′ and ε″ were calculated, were obtained directly from the bridge. The samples took the form of discs 58 mm in diameter and 3 mm thick. Calibration of the apparatus was carried out using standard samples (Trolitul, glass, and air) that were 3 mm thick; the accuracy of ε′ was ±1% and that of ε″ was ±2%. The measurements were carried out at temperatures ranging from 30 to 100°C using an ultrathermostat.

Electrical conductivity measurements

The electrical conductivities (σ) of the investigated samples were measured by the application of Ohm's law using the NFM/5T test cell. A power supply unit (GM 45161/01) from Philips (Amsterdam, the Netherlands) was used. The potential difference V between the plates holding the samples and the current I flowing through it was measured by a multimeter (type URI 1050) from Rohde and Schwarz (Munich, Germany). The electrical conductivity was calculated using the equation:

$$\sigma = dI/AV\Omega^{-1}\mathrm{m}^{-1} \quad (1)$$

where d is the thickness of the sample in meters and A is its surface area in square meters.

The measurements of mechanical properties

Tensile strength, elongation (%), and Young's modulus were measured using an Instron testing machine (model 1026) at 23 ± 2°C with a crosshead speed of 100 mm/min, a chart speed of 200 mm/min, and a load cell range of 0-500 Neuton full scale according to ASTM D 638.77a.[17] The dimensions of the sample were 3 mm in thickness, 4 mm in width, and 20 mm in length. The mean value of five measurements for each sample was taken. The results are given in Table III.

X-ray diffraction measurements

XRD patterns were obtained using a Siemens (Berlin, Germany) D500 diffractometer with a back monochromator and a Cu anticathode (step: 0.02°, step time: 1s, Temp.: 25°C). Special attention was paid to the low 2θ region for accurate determination of d_{001} (i.e., the organoclay d-spacing).

Scanning electron microscopy testing

Phase morphology was studied using a JSM-T20 (JEOL, Tokyo, Japan) scanning electron microscope (SEM). For scanning electron observations, the surface of the polymer was mounted on a standard specimen stub. A thin coating ($\sim 10^{-6}$ m) of gold was deposited into the polymer surface and attached to the stub prior to SEM examination in the microscope to avoid electrostatic charging during examination.

RESULTS AND DISCUSSION

Thermogravimetric analysis

The thermal stabilities of the prepared composites were studied using a thermogravimetric analyzer (TGA). The thermogravimetric behavior could be used as a proof of the interactions between the organic medium and the inorganic nanoplatelets surfaces. The results of TGA analyses of pristine PVC and PVC/organoclay nanocomposites containing 5 and 10 wt % of organoclay are shown in Figures 4–8. The thermal stabilities of plasticized PVC and its composites using the TGA thermograms show that they are stable with no weight loss up to 100°C. The degradation in plasticized PVC and its composites using Cloisite Na^+ (5 wt %), Cloisite 93A (5 wt %), Cloisite 30B (5 wt %), Cloisite Na^+ (10 wt %), Cloisite 93A (10 wt %), and Cloisite 30B (10 wt %) starts above 100°C and continues up to 526.33, 531.02, 539.07, 548.48, 526.40, 528.97, and 532.91°C, respectively. The thermal stabilities of virgin PVC and its composites from the TGA thermograms show that, in the temperature range 235–255°C, the PVC/organoclay nanocomposites contain an organic assist agent that degrades slightly faster than pure PVC. This is because the organic molecules tend to degrade before the PVC, causing a slight weight loss in the nanocomposites. Meanwhile, it was found that the onset temperature of thermal degradation decreases with increasing organoclay loading, because the amount of assist agent used increases with the amount of organoclay in PVC. As a result, the thermal resistances of the PVC/organoclay nanocomposites are lower than that of neat PVC during the first stage. The degradation temperatures listed above also show that during the last stage, after complete degradation of the assist agent, the nanocomposites containing 5 wt % of clay display higher thermal resistances than that of plasticized PVC in the temperature range above 500°C due to the barrier effect arising from the dispersion of the clay platelets[18] and that at higher filler content (10 wt%), the thermal stabilization is less efficient, probably as a result of a less optimal platelet dispersion (steric hindrance). The presented data show that the temperature of degradation

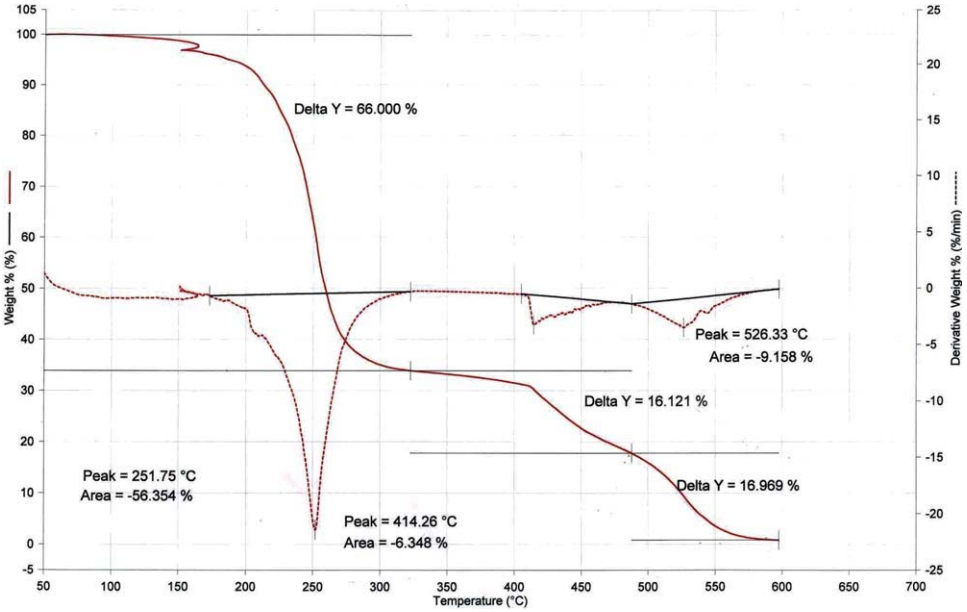

Figure 4 TGA of plasticized PVC. [Color figure can be viewed in the online issue, which is available at wileyonlinelibrary.com.]

is shifted towards a higher value when organophilic MMT is used compared with the polar clay. Thus, it could be concluded that organophilic treatment improves the thermal stability of PVC/clay nanocomposite, due to better interactions between PVC matrix and clay in the sequence: Cloisite Na^+ < Cloisite 93A< Cloisite 30B. The less thermal stability found for the composite containing nanofiller 93A than for that containing nanofiller 30B arises from the fact that Cloisite 93A contains a ternary ammonium salt which is less thermally stable than quaternary ammonium salt present in the interlayer space of Cloisite 30B.[19]

Electrical properties

Although polymer nanocomposites have been found to possess enhanced thermal stabilities, mechanical strengths, corrosion resistance, and fire-retarding and gas-barrier properties; their electrical properties have been ignored in research and so data in the literature on this subject are limited (there are only few of them).[20] Therefore, the present article will focus on studying the dielectric measurements of the PVC nanocomposites to modify selected properties for specific applications.

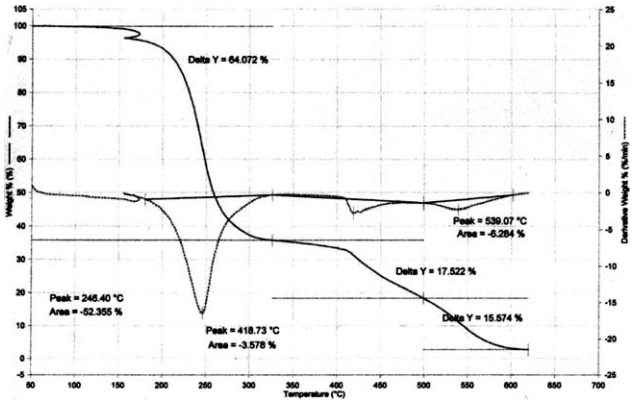

Figure 5 TGA of plasticized PVC/5 wt % Cloisite 93A nanocomposite.

Dielectric characterization

As was stated in the "Experimental" section, the permittivity (ε′) and the dielectric loss (ε″) values of the prepared composites were investigated in the frequency region from 100 Hz to 100 kHz at temperatures of 30–100°C. It is evident from Figure 9, which shows the variations in the values of the ε′ with frequency (*f*) at different temperatures for plasticized PVC and its composites containing 5 and 10 wt % of Cloisite 93A, for an example, that ε′ increases with increasing temperature and decreases with increasing frequency. Similar behavior was noted previously in the literature.[21–25] The increase in ε′ with temperature can be explained by the increased polar group mobility, decreased density, and hence, the decreased effect of the environment which facilitates the orientation of the mobile groups as the temperature increases. The decrease in ε′ with frequency may be caused by dielectric dispersion. Moreover, Figure 9 shows that the value of ε′ decreases with increasing filler content from 5 to 10 wt %, especially in the very low frequency region.

It is also apparent from Figure 10, which represents the variation of ε″ with frequency at different temperatures for plasticized PVC and its composites containing 5 and 10 wt % of Cloisite 93A, that the

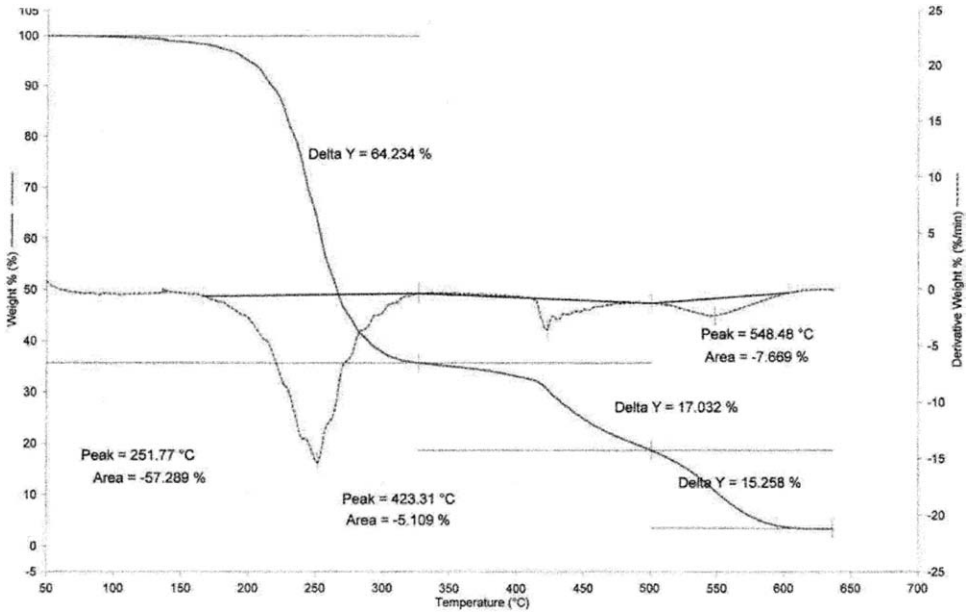

Figure 6 TGA of plasticized PVC/5 wt % Cloisite 30B nanocomposite.

value of ε'' increases at higher temperatures, and it does so especially rapidly in the very low frequency region. Moreover, Figure 10 reveals that, at each temperature, ε'' decreases with increasing filler content from 5 to 10 wt % in the lower frequency region. The low-frequency losses may be due to either dielectric current (dc) conductivity[26,27] resulting from the increase in ion mobility or the Maxwell-Wagner effect[28] resulting from an alternating current (ac) in phase with the applied potential, or to both. To confirm this, the dc conductivities of the investigated samples were measured by application of Ohm's law to the dc flowing through the samples at 200 V and at temperatures from 30 to 100°C. All investigated samples showed appreciable dc conductivity. The dielectric losses due to the dc conductivity (σ) at the different frequencies (ω) are calculated using the following equation[29]:

$$\varepsilon''_{dc} = 9 \times 10^{11}\, 4\Pi\sigma/\omega \qquad (2)$$

where $\omega = 2\Pi f$, and subtracted from the values of ε'' in the low-frequency region. The data of ε'' after subtracting ε''_{dc} are plotted versus log f and are represented in Figure 10. From this figure, it could be concluded that the low-frequency losses are not totally dc losses and that they may comprise Maxwell-Wagner

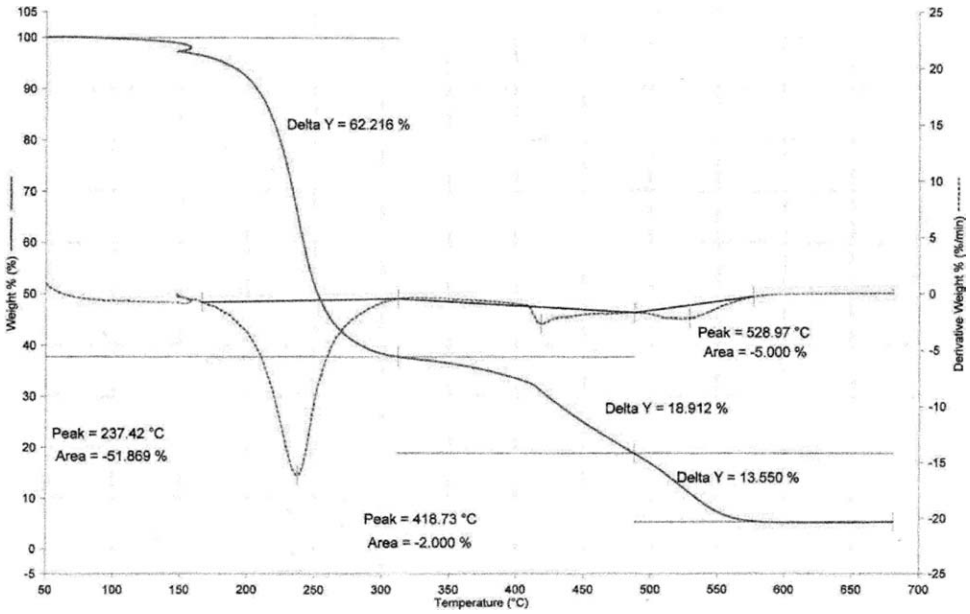

Figure 7 TGA of plasticized PVC/10 wt % Cloisite 93A nanocomposite.

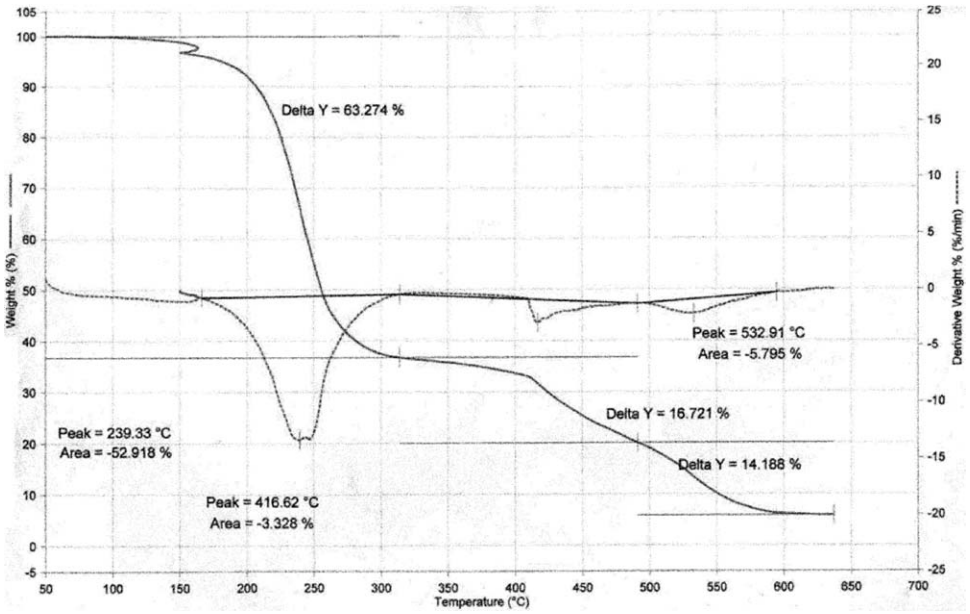

Figure 8 TGA of plasticized PVC/10 wt % Cloisite 30B nanocomposite.

losses, because the differences between the permittivities and conductivities of the different ingredients in the investigated samples are relatively large.

Electrical conductivity

One of the interesting features of electrical conductivity is its temperature dependence, which allows us to understand conduction mechanisms in materials. Figure 11 shows the temperature dependences of the electrical conductivities of plasticized PVC and the composites containing Cloisite Na^+, Cloisite 30B or Cloisite 93A. It is evident from this figure that the electrical conductivity (σ) of plasticized PVC and these composites increases with increasing temperature from 30 to 100°C due to the increased

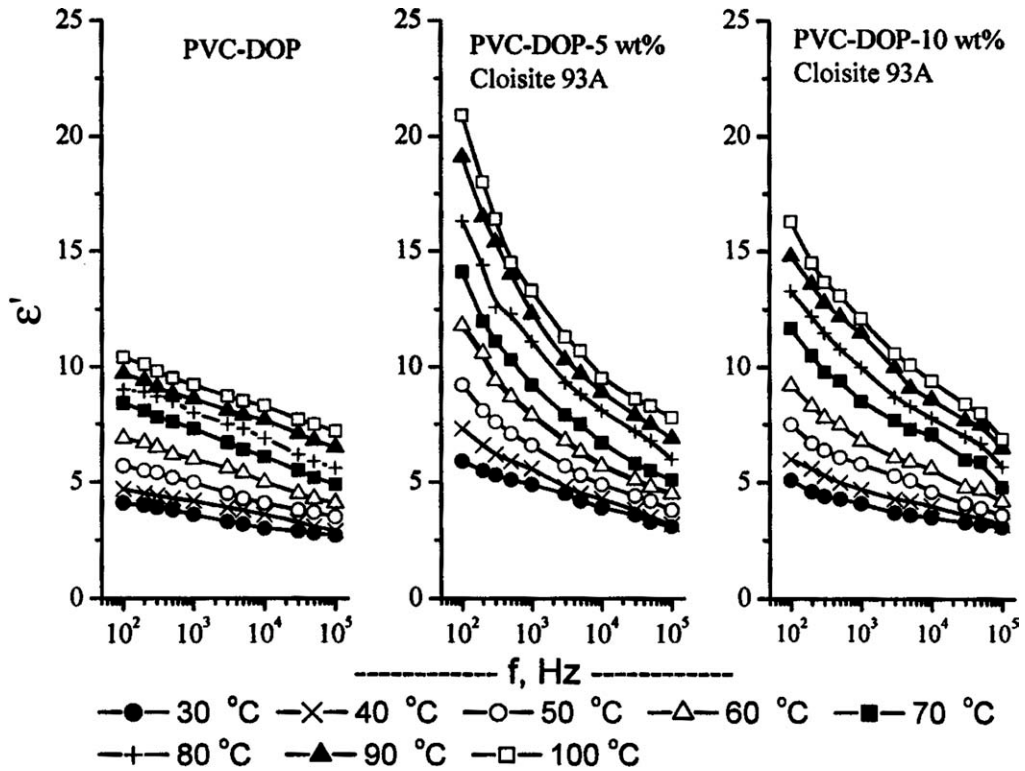

Figure 9 The permittivity (ε') versus frequency (f) for PVC-DOP mixed with Cloisite 93A.

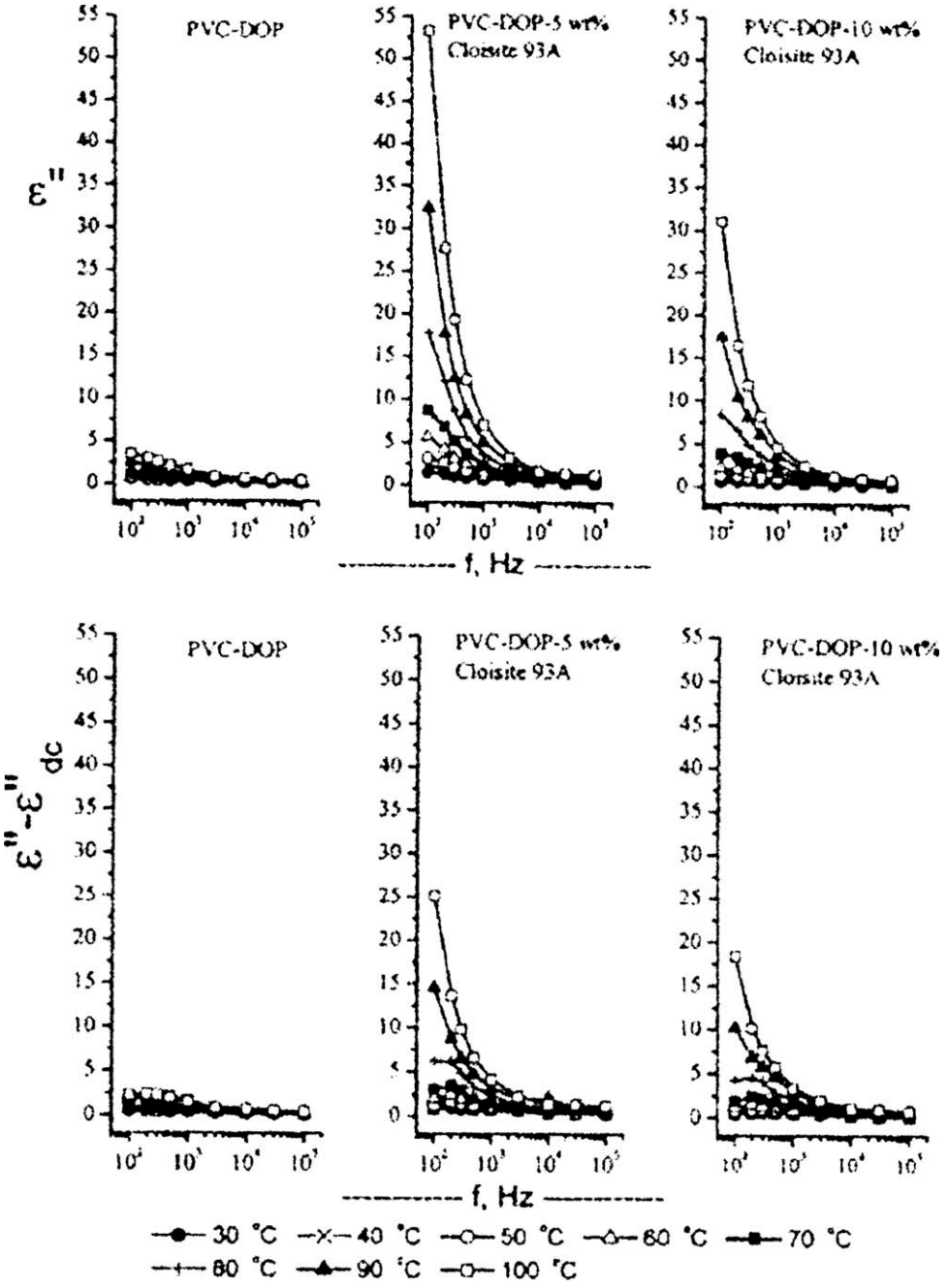

Figure 10 The dielectric loss (ε″) and (ε″- ε''_{dc}) versus frequency (f) for PVC-DOP mixed with Cloisite 93A.

mobilities of ionic bodies that occur as a result of excitation by heating. This characterizes semiconductor-like conduction in these composites. Furthermore, Figure 11, which quantitatively summarizes the data presented in Table I, shows a pronounced increase in the value of σ of plasticized PVC at clay content of 5 wt %, especially in the lower frequency region and at higher temperatures in the sequence : Cloisite Na^+< Cloisite 30B< Cloisite 93A. The obtained values are situated between the two extremes of those of semiconductors ($10^{-10} - 10^{+2}\ \Omega^{-1}\ cm^{-1}$).[30] At 10 wt % content of the filler, the values of σ decrease to some extent. This may be attributed to the formation of some nanoparticle agglomerates due to more intense interfacial interactions between nanoparticles upon further increasing the content of the filler, which may cause some steric hindrance that partially contributes to decreasing the electrical charge mobility.

Different conduction mechanisms are possible in polymers.[31,32] Almost all of the mechanisms are related to different types of polarization that can occur in the system. Each of these mechanisms predominates for a given temperature range and applied electric field.

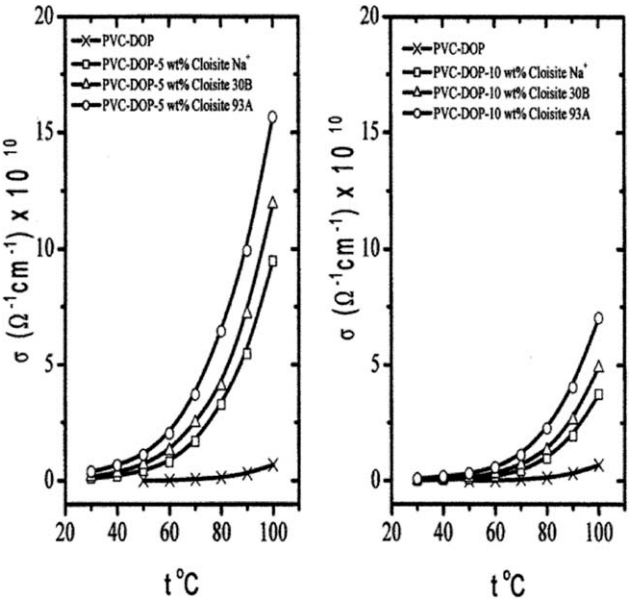

Figure 11 The relation between electrical conductivity (σ) and temperature (*t*) for PVC-DOP mixed with Cloisite Na^+, Cloisite 30B, and Cloisite 93A.

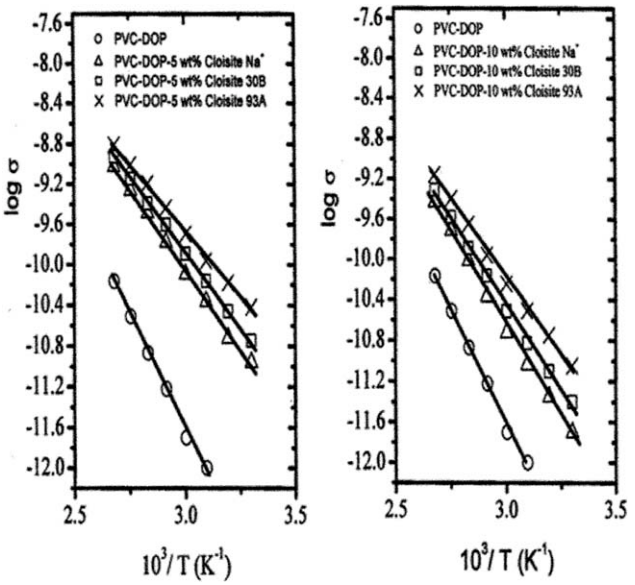

Figure 12 The relation between log σ and $10^3/T$ for PVC-DOP mixed with Cloisite Na^+, Cloisite 30B, and Cloisite 93A.

Activation energy of interaction of PVC with nanoclay

The activation energy (*E*) of the interaction of plasticized PVC with nanoclay was calculated by plotting the logarithm of the conductivity (σ) versus the reciprocal of the absolute temperature (*T*) where a straight line was obtained, as shown in Figure 12. The results indicate that the PVC composites of Cloisite Na^+, Cloisite 30B, or Cloisite 93A tend to behave as semiconductors. From the slope of the straight line, E was calculated using the equation[33]:

$$\sigma = \sigma_o \cdot e^{-E/RT} \tag{3}$$

It has been found that the period of excitation depended on the activation energy needed to make the substance conducting. If the activation energy is low i.e., the system is easily excited, the PVC composite becomes semiconducting at room temperature or in the presence of indirect light. Hence, it can be used for electronic devices working at ambient temperature. It is apparent from Table II that the activation energy of plasticized PVC decreases at the clay content of 5 wt % and decreases to a lesser extent at 10 wt % content of the filler in the sequence: Cloisite Na^+ < Cloisite 30B< Cloisite 93A. The lowest value of the activation energy for PVC/5 wt % Cloisite 93A nanocomposite (5.30 K cal/mol) indicates that it is easily excited and tends to behave as a semiconductor, so can be better employed for electronic and microwave nanodevices.

Mechanical measurements of particle dispersion in PVC nanocomposites

The dispersion of fillers in a polymer matrix has a significant effect on the mechanical properties of composites.[34,35] When the filler size decreases to the nanometer scale, the dispersion process becomes important because the nanoparticles have a strong tendency to self-agglomerate.

Mechanical properties tests (tensile strength, elongation (%), and Young's modulus) were performed on

TABLE I
Electrical Conductivity of PVC-DOP Mixed with 5 and 10 wt % of Cloisite Na^+, Cloisite 30B, or Cloisite 93A

Samples	σ × 10^{10} (Ω^{-1} cm^{-1}) at temperatures (°C)							
	30	40	50	60	70	80	90	100
PVC-DOP	–	–	0.01	0.02	0.06	0.14	0.31	0.68
PVC-DOP-5 wt % Cloisite Na^+	0.11	0.19	0.43	0.80	1.67	3.27	5.47	9.48
PVC-DOP-5 wt % Cloisite 30B	0.18	0.35	0.69	1.28	2.49	4.07	7.19	11.95
PVC-DOP-5 wt % Cloisite 93A	0.38	0.66	1.09	2.01	3.70	6.44	9.92	15.65
PVC-DOP-10 wt % Cloisite Na^+	0.02	0.05	0.09	0.19	0.43	0.97	1.93	3.73
PVC-DOP-10 wt % Cloisite 30B	0.04	0.08	0.15	0.31	0.69	1.30	2.63	4.89
PVC-DOP-10 wt % Cloisite 93A	0.09	0.18	0.31	0.57	1.10	2.25	4.03	7.02

TABLE II
Activation Energy of PVC-DOP Mixed with 5 and 10 wt % of Cloisite Na^+, Cloisite 30B, or Cloisite 93A

Samples	Activation energy (Kcal/mol)
PVC-DOP	9.13
PVC-DOP-5 wt % Cloisite Na^+	6.39
PVC-DOP-5 wt % Cloisite 30B	5.90
PVC-DOP-5 wt % Cloisite 93A	5.30
PVC-DOP-10 wt % Cloisite Na^+	7.65
PVC-DOP-10 wt % Cloisite 30B	7.21
PVC-DOP-10 wt % Cloisite 93A	6.45

PVC/MMT nanocomposites with MMT loadings of 5 and 10 wt %, and the results are listed in Table III. The presented data show that the tensile strength, elongation (%), and Young's modulus of the three PVC/MMT nanocomposites are increased significantly at 5 wt % of MMT loading in the sequence :Cloisite Na^+< Cloisite 93A < Cloisite 30B. In this respect, at 5 wt % content of nanofiller, the interfacial interaction between the nanoparticles and the PVC matrix increases, this causes the nanoparticle agglomerates to break down, enhances the dispersion of the nanoparticles in the PVC, and improves the interfacial adhesion between the nanparticles and the PVC matrix. Increasing the nanoparticle loading further, to 10 wt %, in the nanocomposites results in a deterioration in the tensile strength, elongation (%), and Young's modulus in the sequence: Cloisite Na^+ < Cloisite 93A< Cloisite 30B; although the composites still show good ductility. At higher degrees of loading, the nanoparticles tend to interact to form nanoparticle agglomerates rather than to interact with the PVC matrix, leading to poor interfacial adhesion between the PVC and the filler phases, and to a subsequent deterioration in the crosslinking across the interfaces. The decrease in the elongation (%) may be due to an interstructural process in which the filler molecules are distributed in the interaggregate space.

It is important to point out that TGA and mechanical measurements prove that organophilic clays are better candidates, compared to chemically untreated natural clay, for achieving a dispersed state, thus leading to an improvement in the nanocomposites' final properties, such as its thermal stability and mechanical behavior.[19] This is because the nanoscale Cloisite Na^+ layers have high specific surface area and surface energy, which makes them tend to aggregate together rather than to disperse homogeneously in PVC matrix, especially at high MMT loadings.[36]

Morphologies of the PVC/organoclay nanocomposites

The nanocomposites were analyzed by X-ray diffraction (XRD) and scanning electron microscopy (SEM) to estimate the degree of dispersion of the organoclay particles in the polymer matrix.

XRD analysis

X-ray diffraction is the method most commonly used to assess the morphology of the nanoclay in either powder form or when compounded into a polymer matrix. The X-rays are reflected from each clay layer within a sample, so there is a relationship between the angle θ and the physical spacing in the system. At small angles, the diffraction peak position is related to the interlayer spacing according to Bragg's law: $\lambda = 2\ d \sin\theta$, where λ is the wavelength of the X-rays used, d is the spacing between the diffraction planes and θ is the measured diffraction angle. One of the limitations of X-ray diffraction analysis is that it may not always yield a unique interpretation of the data. Often, other techniques must be used to complement the diffraction experiments.[37] XRD characterization is generally based on a comparison between the diffraction peak position of the nanoclay powder and that of the nanoclay in the polymer matrix.[38]

When MMT is modified by organic modifier, the gallery of MMT is intercalated and expanded by the molecular chain of the organic modifier. The XRD pattern of Cloisite 30B shows a characteristic diffraction peak (d_{001} plane) at $2\theta = 5.296^\circ$, corresponding to basal spacing of 16.672 Å [Fig. 13(a)] while the XRD pattern of Cloisite 93A exhibits a characteristic diffraction peak (d_{001} plane) at $2\theta = 3.967$, corresponding to basal spacing of 22.257 Å [Fig. 14(a)].

In compounded samples, the increased clay spacing due to the addition of the plasticized PVC between the platelets is evident. The gallery spacing of organoclay in polymer nanocomposites generally depends on the interaction beween the polymer

TABLE III
Mechanical Properties of PVC-DOP Mixed with 5 and 10 wt % of Cloisite Na^+, Cloisite 93A, or Cloisite 30B

Samples	Tensile strength (N/mm)	Elongation (%)	Young's modulus (N/mm)
PVC-DOP	17.12	35.74	47.80
PVC-DOP-5 wt % Cloisite Na^+	22.10	45.95	62.02
PVC-DOP-5 wt % Cloisite 93A	25.01	59.45	71.34
PVC-DOP-5 wt % Cloisite 30B	29.02	89.37	90.92
PVC-DOP-10 wt % Cloisite Na^+	17.84	36.85	50.13
PVC-DOP-10 wt % Cloisite 93A	18.91	40.46	56.10
PVC-DOP-10 wt % Cloisite 30B	21.25	58.58	66.05

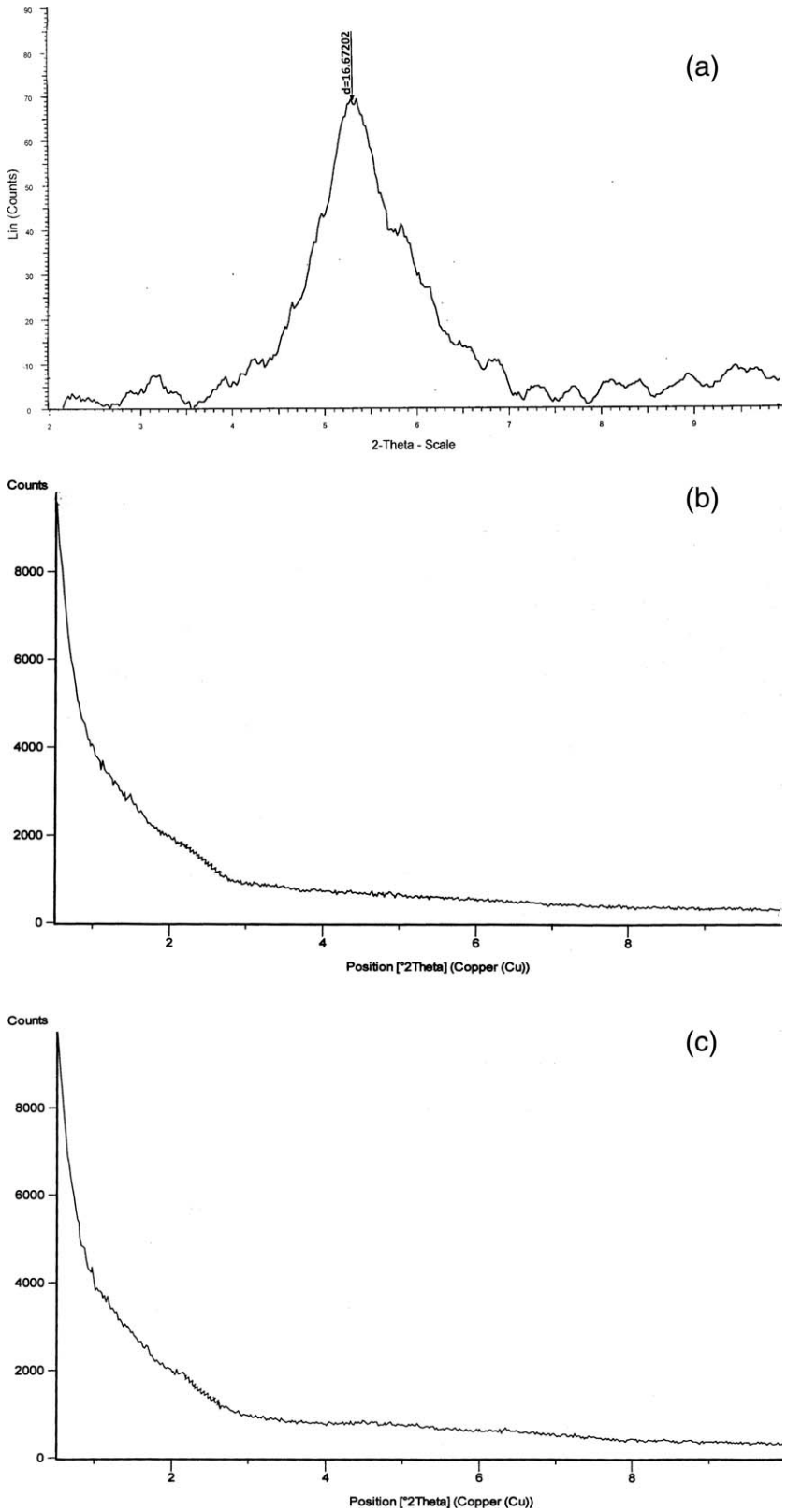

Figure 13 (a) XRD pattern of Cloisite 30B. (b) XRD pattern of PVC/5 wt % Cloisite 30B nanocomposite. (c) XRD pattern of PVC/10 wt % Cloisite 30B nanocomposite.

matrix and the organoclay.[39,40] The XRD patterns of Cloisite 30B and the PVC/organoclay nanocomposites with 5 and 10 wt % of Cloisite 30B are shown in Figure 13(a–c) and those of Cloisite 93A and the PVC/organoclay nanocomposites with 5 and 10 wt % of Cloisite 93A are shown in Figure 14(a–c). For

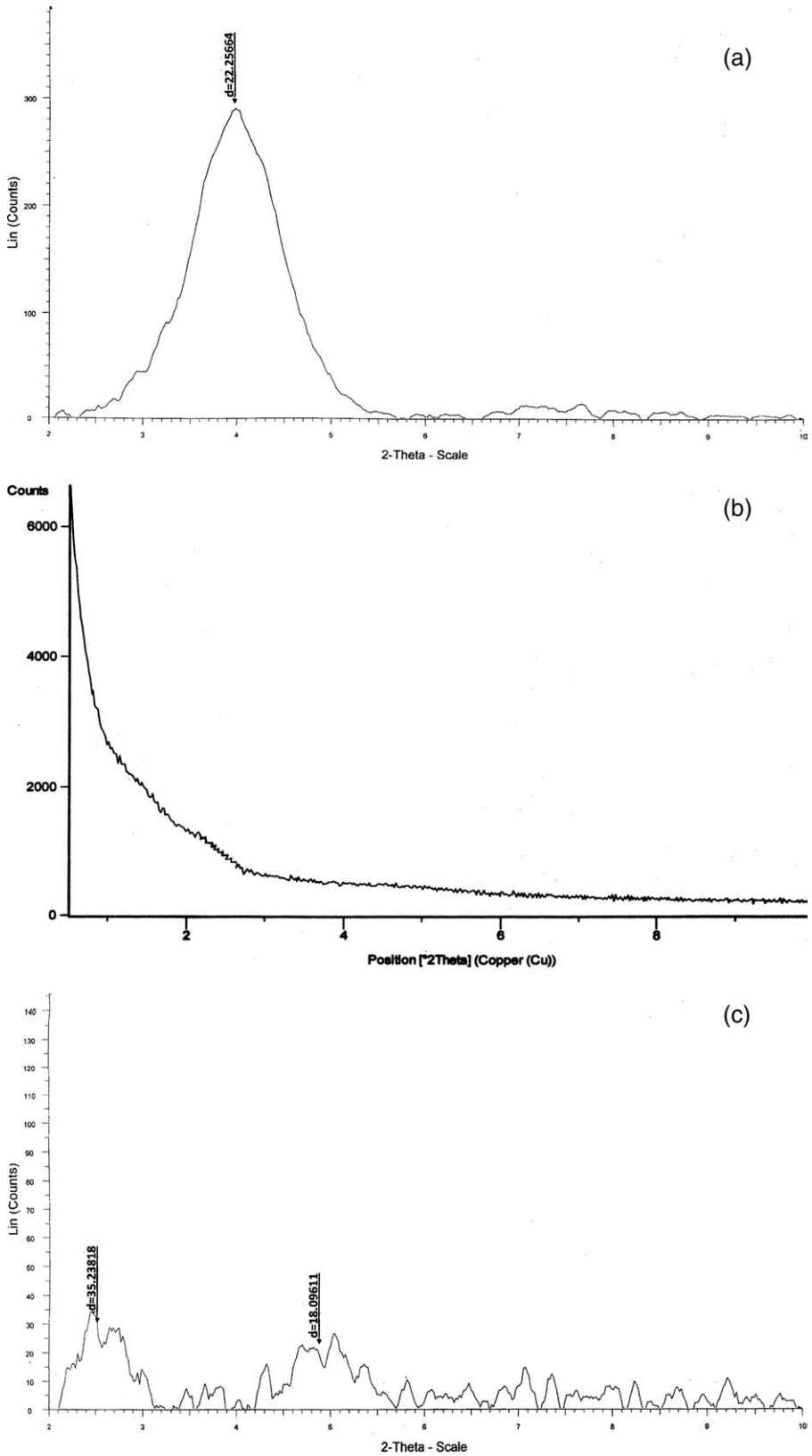

Figure 14 (a) XRD pattern of Cloisite 93A. (b) XRD pattern of PVC/5 wt % Cloisite 93A nanocomposite. (c) XRD pattern of PVC/10 wt % Cloisite 93A nanocomposite.

PVC/5 and 10 wt % Cloisite 30B nanocomposites, the diffraction peak from the (d_{oo1} plane) of Cloisite 30B is completely disappeared, implying that most of the organoclay platelets is successfully exfoliated and well dispersed in the PVC matrix, and thus form delaminated nanocomposites.[35,41] Furthermore,

for PVC/5 wt % Cloisite 93A nanocomposite, the diffraction peak from the (d_{oo1} plane) of Cloisite 93A is completely disappeared while for PVC/10 wt % Cloisite 93A nanocomposite, the shift of this diffraction peak to $2\ominus = 2.505^\circ$ shows an increase in the interlayer spacing from 22.257 Å to 35.238 Å indicating that this nanocomposite has a low level of exfoliation of the clay in PVC matrix and that the PVC molecular chains are most likely intercalated and expanded into the galleries of silicate layers to form a multilayered structure consisting of layers of PVC molecular chains alternating with layers of layered silicate.[42,43]

SEM characterization

Further evidence of the nanometer-scale dispersion of silicate layers in PVC/organoclay nonocomposites is provided by SEM micrographs. Figure 15 shows SEM micrographs of plasticized PVC-0 (a) and PVC/5 and 10 wt % Cloisite 30B nanocomposites: PVC-5(b) and PVC-10(c). Figure 16 also shows SEM micrographs of plasticized PVC-0(a) and PVC/5 and 10 wt % Cloisite 93A nanocomposites: PVC-5 (d) and PVC-10 (e). Figures 15(b) and 16(d) show SEM micrographs of PVC/5 wt % Cloisites 30B and 93A nanocomposites, respectively, and reveal that the organoclay layers are homogeneously dispersed in the PVC matrix,[44] suggesting greater interactions between the organoclay nanoparticles and the polymeric chains, and there is no evidence of huge agglomerates. In contrast, when the organoclay content is 10 wt %, the nanoparticles are very closely surrounded by their neighbors and agglomerates form [Figs. 15(c) and 16(e)].

In conclusion, the interaction between the PVC and the organoclay is an important factor in the morphological development of PVC/organoclay nanocomposites.

CONCLUSIONS

The thermal stabilities, electrical conductivities, and tensile properties of PVC/Cloisite Na^+, Cloisite 30B, and Cloisite 93A nanocomposites have been investigated in this study, with the aim being to control the dispersibility of nanoclay in PVC matrix. The obtained results lead to the following conclusions:

- The Organic modifiers of Cloisites 30B and 93A lower the surface energy of the silicate layers and enhance the miscibility between the silicate layers and the polymer matrix.
- The thermal stability and mechanical properties of plasticized PVC are enhanced by introducing Cloisite Na^+, Cloisite 93A, and Cloisite 30B at 5 wt% in the sequence: Cloisite Na^+ < Cloisite 93A< Cloisite 30B.

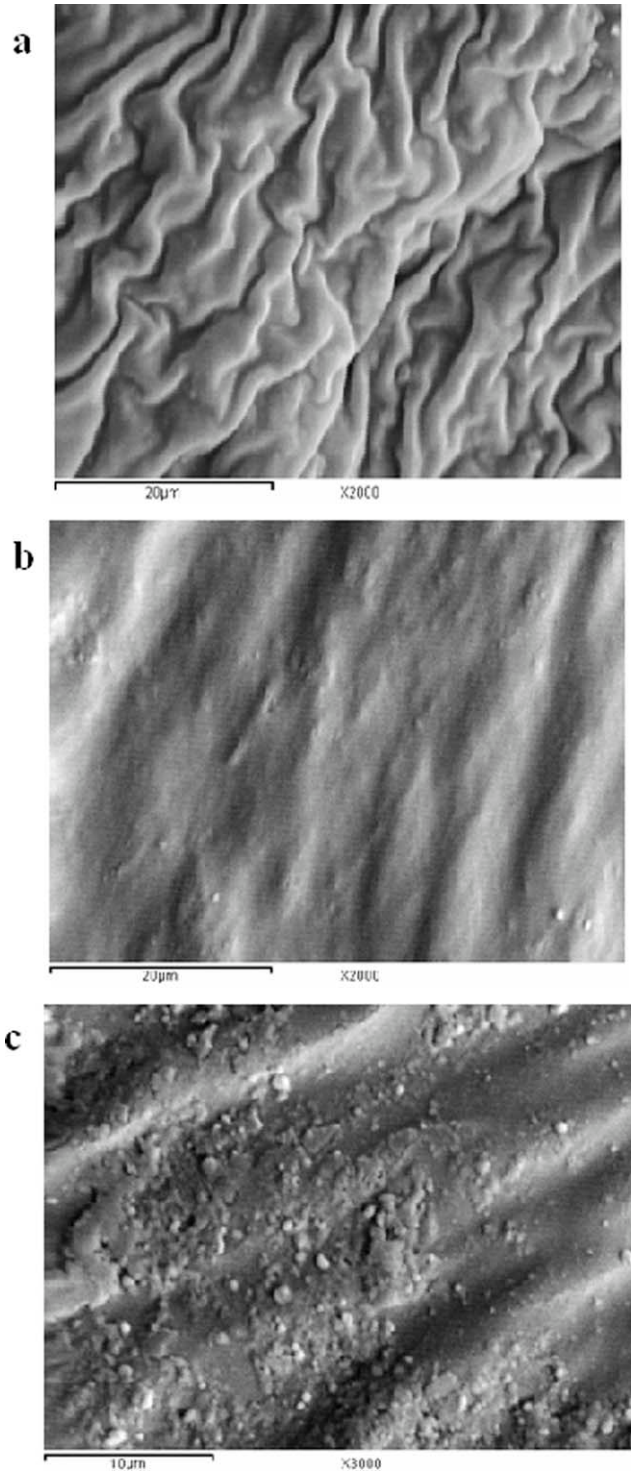

Figure 15 SEM micrographs. PVC-0 (a), PVC-5 (b), PVC-10 (c).

- The permittivity and dielectric loss increase with increasing temperature and decrease with increasing frequency, especially at the very low frequency region; and also increase by introducing Cloisite Na^+, Cloisite 30B, and Cloisite 93A at 5 wt %.
- The electrical conductivity of plasticized PVC is enhanced by introducing Cloisite Na^+, Cloisite 30B, and Cloisite 93A at 5 wt % in the sequence:

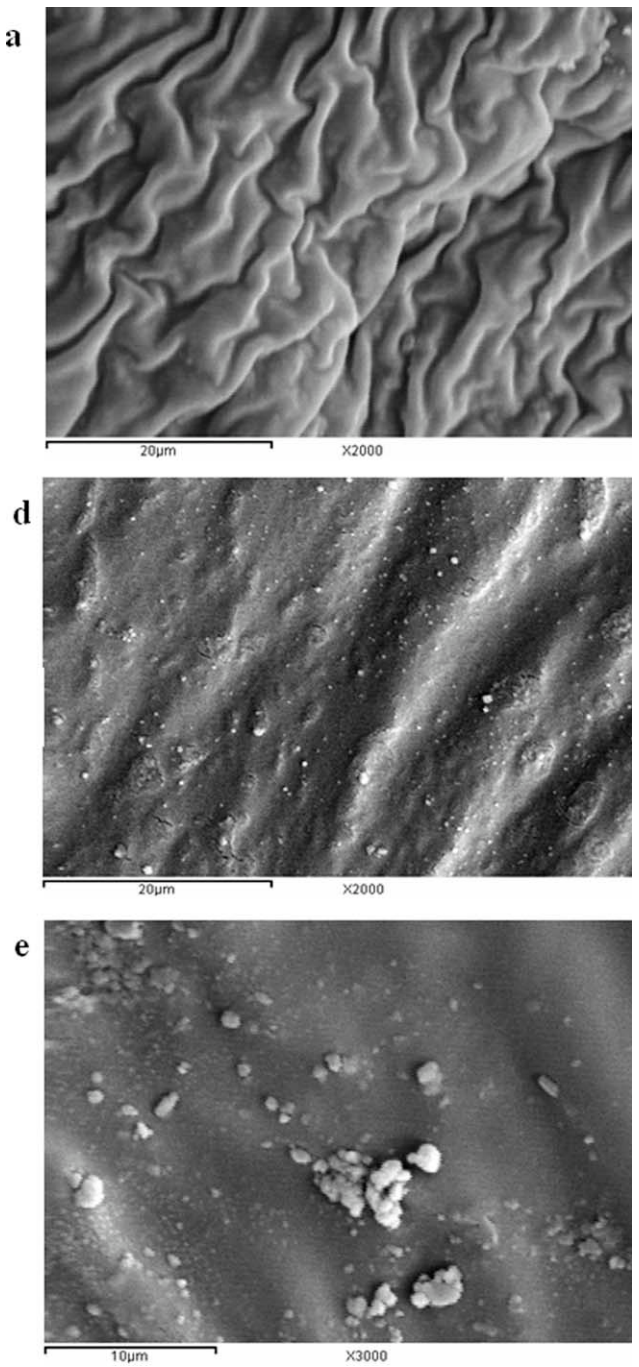

Figure 16 SEM micrographs: PVC-0 (a), PVC-5 (d), PVC-10 (e).

Cloisite Na^+ < Cloisite 30B < Cloisite 93A. The temperature dependence of the conductivity shows that the prepared composites are semiconductor-like.

- The activation energy of interaction of PVC with nanoclay is determined by measuring electrical conductivities and found lowest for the composite containing 5 wt % of clay, showing that it is easily excited and can be employed for electronic and microwave nanodevices as a semiconductor.

Studies of XRD and SEM analyses confirm that the particles of Cloisites 30B and 93A are successfully dispersed in PVC matrix.

The authors express their many thanks and deep gratitude to ICCM-16 and the JSCM for their great cooperation.

References

1. Rothon, R. Particulate-Filled Polymer Composites, 1st ed. Longman Scientific: Harlow, 1995.
2. Fukushima, Y.; Inagaki, S. J Inclusion Phenomena 1987, 5, 473.
3. Okada, A.; Kawasumi, M.; Kurauchi, T.; Kamigaito, O. Polym Preparation 1987, 28, 447.
4. Boucard, S.; Duchet, J.; Gerard, J. F.; Prele, P.; Gonzalez, S. Macromol Symp 2002, 194, 241.
5. Alexandre, M.; Dubois, P. Mater Sci Eng 2000, 28, 1.
6. Pinnavaia, T. J.; Beall, G. W. Polymer-Clay Nano-Composites; John Wiley & Sons, Inc, 2000.
7. Glanellis, E. P. Adv Mater 1996, 8, 29.
8. Bharadwaj, R. K. Macromolecules 2001, 34, 9189.
9. Beyer, G. Fire Mater 2001, 25, 193.
10. Berlund, L. Filler Additives Plast 2000, 4, 31.
11. Leykin, A.; Loelovich, M.; Figovsky, O. Eurofillers 2003 International Conferenc, Alicante (SPAIN) September 8–11, P363, 2003.
12. Jeziórska, R.; Klepka, T.; Paukszta, D. Polimery (Warsaw) 2007, 52, 294.
13. Zhang, Y. H.; Gong, K. C. Mater Res Soc 1998, 520, 191.
14. Wang, D. Y.; Parlow, D.; Wilkie, C. A. Polym Prepr 2001, 42, 842.
15. Trlica, J.; Kalendova, A.; Malac, Z.; Simonik, J.; Pospisil, L. ANTEC 01 Conference, Dallas, USA, 6–10 May, pp. 2162–2165, 2001.
16. Mackenzie, R. C. The Differential Thermal Investigation of Clays; Mineralogy Society: London, 1957.
17. American Society for Testing Materials (ASTM), ASTM D 638.77a, ASTM, Philadelphia, PA, 1980.
18. Zanetti, M.; Camino, G.; Thomann, R.; Mulhaupt, R. Polymer 2001, 42, 4501.
19. Peprnicek, T.; Duchet, J.; Kovarova, L.; Malac, J; Gerard, J. F.; Simonik, J. Polym Degrad Stab 2006, 91, 1855.
20. Dong, X.; Zhou, G.; Zhang, J. Fangzhi Xuebao 2004, 25, 16.
21. Saad, A. L. G.; Hassan, A. M.; Gad, E. A. M. J Appl Polym Sci 1993, 49, 1725.
22. Saad, A. L. G.; Hassan, A. M.; Youssif, M. A.; Ahmed, M. G. M. J Appl Polym Sci 1997, 65, 27.
23. Saad, A. L. G.; Hussien, L. I.; Ahmed, M. G. M.; Hassan, A. M. J Appl Polym Sci 1998, 69, 685.
24. Saad, A. L. G.; Sayed, W. M.; Ahmed, M. G. M.; Hassan, A. M. J Appl Polym Sci 1999, 73, 2657.
25. Saad, A. L. G.; Aziz, H. A.; Dimitry, O. I. H. J Appl Polym Sci 2004, 91, 1590.
26. Hanna, F. F.; Yehia, A. A.; Abou Bakr, A. Br Polym 1973, 5, 83.
27. Davies, J. M.; Miller, R. F.; Busse, W. F. J Am Chem Soc 1941, 63, 361.
28. Sasabe, H.; Saito, S. J. J Polym Sci Part A: Polym Chem 1969, 2, 7, 1405.
29. Smyth, C. P. Dielectric Behaviour Structure; McGraw-Hill: New York, 1955.
30. Goodings, E. P. Chem Soc Revs 1976, 5, 95.
31. Kemeny, G.; Mahanti, S. D. Proc Natl Acad Sci USA 1975, 72, 999.
32. Pochtennyi, A. E.; Ratnikov, E. V. Dokl Akad Nauk Bssr 1981, 25, 896.

33. Eley, D. D.; Partfitt, G. D. Trans Faraday Soc 1955, 51, 1529.
34. Choi, W. J.; Kim, S. H.; Kim, Y. J.; Kim, S. C. Polymer 2004, 45, 6045.
35. Jeong, E. H.; Yang, J.; Hong, J. H.; Kim, T. G.; Kim, J. H.; Youk, J. H. Eur Polym J 2007, 43, 2286.
36. Wan, C.; Qiao, X.; Zhang, H. Polym Test 2003, 22, 453.
37. Marton, E.; Marton, C. Methods of Experimental Physics, 16-Part B, Chpt. 6.7, 1980.
38. Manias, E.; Touny, A.; Wu, L.; Strawhecker, K.; Lu Chung, T. C. Chem Mater 2001, 13, 3516.
39. Oh, S. T.; Ha, C. S.; Cho, W. J. J Appl Polym Sci 1994, 54, 859.
40. Grapski, J. A.; Cooper, S. L. Biomaterials 2001, 22, 2239.
41. Tortora, M.; Gorrasi, G.; Vittoria, V.; Galli, G.; Ritrovati, S.; Chiellini, E. Polymer 2002, 43, 6147.
42. Hu, Y.; Song, L.; Xu, J.; Yang, L.; Chen, Z.; Fan, W. Colloid Polym Sci 2001, 279, 819.
43. Song, L.; Hu, Y.; Tang, Y.; Zhang, R.; Chen, Z.; Fan, W. Polym Degrad Stab 2005, 87, 111.
44. Xie, X. L.; Li, R. K. Y.; Liu, Q. X.; Mai, Y. W. Polymer 2004, 45, 2796.